

Study on Temperature and Thermal Stress of Fused Silica Micropores in Laser Processing

Qi Zhao^{a,*}, Man Peng^a, Anjiang Lu^a, Zhongchen Bai^b

^aCollege of Big Data and Information Engineering, Guizhou University, Guiyang 550025, China

^bKey Laboratory of Optoelectronic Technology and Application, Guiyang 550025, China
 isaaczao0378@163.com

To study the laser processing of fused silica microchannels, the temperature and thermal stress of fused silica micropores irradiated by TEM00, TEM01 and Flat-top three modes were simulated. The morphology of the micropores was analyzed and the simulation results were compared. The results show that the spatial distribution of the laser intensity and the morphology of the micropores would all affect the temperature distribution and stress distribution of the material; the temperature accumulation effect is obvious, and the temperature continues to increase after continuous pulse action, in some mode, under light beam irradiation the focus area temperature exceeds the melting temperature of the material; the temperature gradient results in generating of thermal stress, which can cause damage if it exceeds the mechanical threshold of the material. The simulation results provide a useful reference for fused silica microchannel processing.

1. Introduction

Fused silica has good electro-osmotic property, excellent optical property, high wetting ability, weak surface adsorption and inert surface reaction, and is suitable for use as a MEMS microfluidic chip material. The microchannel is the basic structural unit of the microfluidic chip. During the microchannel processing of fused silica by the laser, melting and vaporization will occur. During the process, measurement of temperature, stress, and deformation inside the fused silica is inconvenient, so we can use modeling and simulation to conduct effective studies.

Theoretical calculations and simulations of temperature and stress distributions of laser-material interactions have yielded many results (Feit, 2002; Norton, 2004; Suratwala, 2011; Suratwala, 2011; Yoshida, 2012). The literature compares the temperature field of CO₂ laser-irradiated fused silica and BK7 glass (Wei et al., 2005); Li et al. (2012) studied the effect of high repetition rate pulses on the temperature cumulative effect; Literature has conducted numerical calculation to the temperature and the thermal stress of the fused silica under the single pulse action (Li, 2016); Yu (2012) analyzed the temperature field, stress field and residual stress distribution of laser-irradiated fused silica; Cai et al. (2014) conducted numerical simulation of the thermal stress of the antireflective silica, Jiao and Wang (2007) studied the temperature distribution of the moving silica glass under the action of CO₂ laser; Su and Zeng (2009) analyzed the thermal stress of the window material under laser irradiation.

For the fused silica microchannel processing, there is a case where a same position is repeatedly processed to form a deeper microchannel. This paper simulates the temperature and thermal stress of fused silica micropores under laser irradiation with TEM00, TEM01 and Flat-top three modes. The simulation results provide useful reference for temperature control, stress control and laser mode selection in the fused silica microchannel laser processing.

2. Basic principles

2.1 Laser heating temperature field equation

Considering that the simulation object is a nanosecond laser pulse, and the pulse and fused silica have a short action time, ignoring silica radiation, and conduction and convection in the surrounding air, the Fourier heat conduction equation is obtained as (Grigoropoulos, 2009):

$$\rho C \frac{\partial T}{\partial t} + \nabla \cdot (-k \nabla T) = Q \quad (1)$$

In the formula, $\nabla \cdot (-k \nabla T)$ is the heat conduction term, Q is the heat source, t is the time, ρ is the density, C is the heat capacity, k is the thermal conductivity, and T is the temperature. Considering that the laser heats quickly, ignoring convection and radiation terms under adiabatic conditions, the boundary conditions are:

$$-\mathbf{n} \cdot (-k \nabla T) = 0 \quad (2)$$

\mathbf{n} is unit vector.

2.2 Thermal stress and strain analysis

The relationship between stress \mathbf{s} , strain $\boldsymbol{\varepsilon}$ and temperature T is known from the generalized Hooke's law (COMSOL, 2013):

$$\mathbf{s} = \mathbf{s}_0 + \mathbf{C} : (\boldsymbol{\varepsilon} - \boldsymbol{\varepsilon}_0 - \boldsymbol{\varepsilon}_h) \quad (3)$$

Where, \mathbf{s}_0 and $\boldsymbol{\varepsilon}_0$ are the initial stress and strain. Strain $\boldsymbol{\varepsilon}$ can be represented by a gradient of deformation $\nabla \mathbf{u}$, as follows:

$$\boldsymbol{\varepsilon} = \frac{1}{2} (\nabla \mathbf{u} + \nabla \mathbf{u}^T) \quad (4)$$

The thermal strain variable $\boldsymbol{\varepsilon}_{th} = \boldsymbol{\alpha}(T - T_{ref})$, $\boldsymbol{\alpha}$ is the expansion coefficient of the material, ":" is the two-point product of the tensor (double-point multiplication), and \mathbf{C} is fourth-order elastic tensor.

3. Simulation calculation

3.1 Silica material selection and environmental conditions

The parameters of fused silica at various temperatures are shown in Table 1 (Yu, 2012). Using piecewise linear function to fit the above physical parameters, parameters below 20°C were replaced by parameters of 20°C, and parameters above 2500°C were replaced by parameters of 2500°C to facilitate simulation calculation. Assuming silica material parameters that do not change with temperature are: absorption coefficient $\beta = 10 \text{ cm}^{-1}$, density $\rho = 2.2 \text{ g/cm}^3$, reflection coefficient $R = 0.035$.

Table 1: Physical parameters of fused silica

Temperature (°C)	Thermal conductivity (W/(m·K))	Heat Capacity (J/(kg·K))	Density (kg/m ³)	Expansion coefficient /10 ⁻⁷ (1/K)	Young modulus (10 ⁹ Pa)	Poisson ratio
20	1.30	740	2200	2.76	71.44	0.158
250	1.56	987	2200	7.95	70.76	0.153
500	1.84	1121	2200	5.75	70.30	0.150
750	2.13	1178	2200	4.68	70.43	0.148
1000	2.40	1121	2200	4.17	71.05	0.150
1500	2.26	1246	2200	5.10	73.79	0.160
1700	2.28	1273	2200	6.00	75.45	0.166
2000	\	\	2200	11.45	85.28	0.21
2500	2.38	1273	2200	11.45	\	\

3.2 Morphology of fused silica micropores

The micropores formed by laser ablation of fused silica are three-dimensional Gaussian fusion pits (Jian, 2012). The contour is approximately expressed as:

$$L(r, \varphi, z) = \begin{cases} L_0 \exp\left(-\frac{r^2}{R_0^2}\right) + C, & r^2 \leq r_0^2 \\ a(r - r_0) \exp[b(r - r_0)], & r^2 > r_0^2 \end{cases} \quad (5)$$

Takes following morphology parameter values of the micropores: $L_0 = 4.47 \times 10^{-5}$; $a = 1.4138$; $b = -2 \times 10^5$; $C = -4.713 \times 10^{-6}$; $r_0 = 1.5 \times 10^{-5}$.

3.3 Laser heating source distribution function

Taking into account that the simulation object is a nanosecond pulse laser, ignoring the time the pulse travels in the material, the laser heat source is expressed as (Grigoropoulos, 2009):

$$Q(r, \varphi, z, t) = (1 - R)\beta P(t)I(r, \varphi, z) \exp[-\beta(z - L(r, \varphi, z))] \quad (6)$$

Where, β is the material absorption coefficient, R is the material reflection coefficient, $P(t)$ is the laser power time distribution, $I(r, \varphi, z)$ is the laser intensity spatial distribution, and $L(r, \varphi, z)$ is the spatial morphology of the fused silica ablation holes.

The simulation uses Gaussian laser pulses, its power form is:

$$P(t) = P_{\max} \exp\left[-4 \ln 2 \left(\frac{t}{t_p}\right)^2\right] = \left(\frac{E_p}{1.064 t_p}\right) \exp\left[-4 \ln 2 \left(\frac{t}{t_p}\right)^2\right] \quad (7)$$

Where P_{\max} is the pulse peak power, E_p is the energy of a single pulse, t_p is the pulse width (FWHM--Full Wave at Half Maximum).

The light intensity distribution of Flat Top beam in cylindrical coordinate system is:

$$I(r, \varphi, z, t) = \begin{cases} \frac{P(t)}{\pi r^2}, & r^2 \leq w_0^2 \\ 0, & r^2 > w_0^2 \end{cases} \quad (8)$$

Where, w_0 is the focal spot radius.

The power density distribution of TEM00 mode Laguerre-Gaussian beam at different positions at different times is (Gao, 2011):

$$I(r, \varphi, z, t) = \frac{2P(t)}{\pi w^2(z)} \exp\left(\frac{-2(r^2)}{w^2(z)}\right) \quad (9)$$

The power density distribution of TEM01 mode Laguerre-Gaussian beam at different positions at different times is (Gao, 2011):

$$I(r, \varphi, z, t) = \frac{2P(t)}{\pi w^2(z)} \cdot \left(1 - \frac{2(r^2)}{w^2(z)}\right) \cdot \exp\left(\frac{-2(r^2)}{w^2(z)}\right) \quad (10)$$

Where, $w(z)$ is the beam radius, $w(z) = w_0 \sqrt{1 + z^2/z_R^2}$, $z_R = n\pi w_0^2/\lambda$ is the Rayleigh length, n is medium refractive index, λ is laser wavelength, and w_0 is focal spot radius.

3.4 Model device

As shown in Figure 1(a), the light beam is irradiated on the upper surface of the cylindrical fused silica with ablative damage, focusing on the center of the damage hole. Adopt acoustic-optical Q-switching Nd: YAG laser parameters, laser wavelength $\lambda = 1064\text{nm}$, pulse energy $E_p = 1.7\text{mJ}$, pulse width (full width at half maximum, FWHM) $t_p = 140\text{ns}$, focal spot radius $w_0 = 20\mu\text{m}$; geometrical shape of fused silica sample is

cylinder, diameter 600 μm , length 500 μm , duration of simulation process is 3.57 μs , including three consecutive laser pulses, the power time distribution is shown in Figure 1(b).

Select 4 sampling points to observe the temperature and stress, point A is at the bottom of the hole (0, -40), point B is at the half height of the hole (7.75, -20), and point C is at the surface where $z=0$ (15, 0), Point D is located at the highest point of the peripheral bulge (20.1, 2.7), unit in micron. As shown in Figure 1(c).

The external surface of the silica is treated with thermal insulation processing; the initial temperature of the fused silica and the ambient temperature are both 293K; the initial values of the displacement field and the velocity field are both 0 m/s. COMSOL software was used to simulate the temperature and thermal stress distribution results.

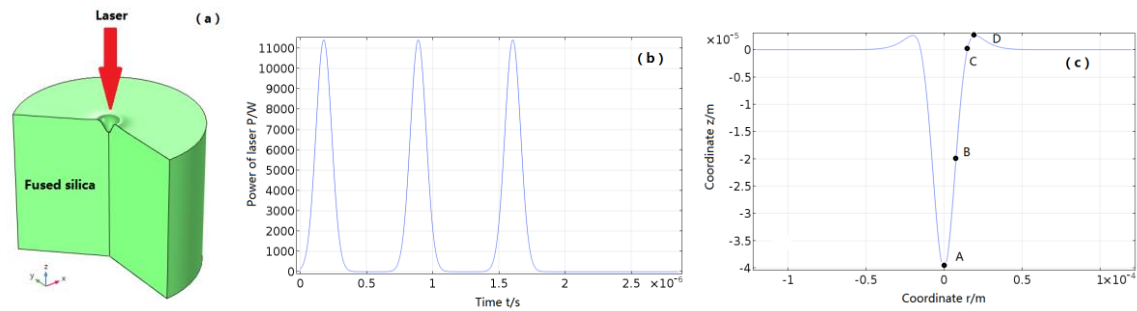


Figure 1: (a) Laser irradiation system (b) Laser power distribution (c) Micropore morphology and adoption points

4. Analysis and discussion

4.1 Temperature and thermal stress distribution of fused silica

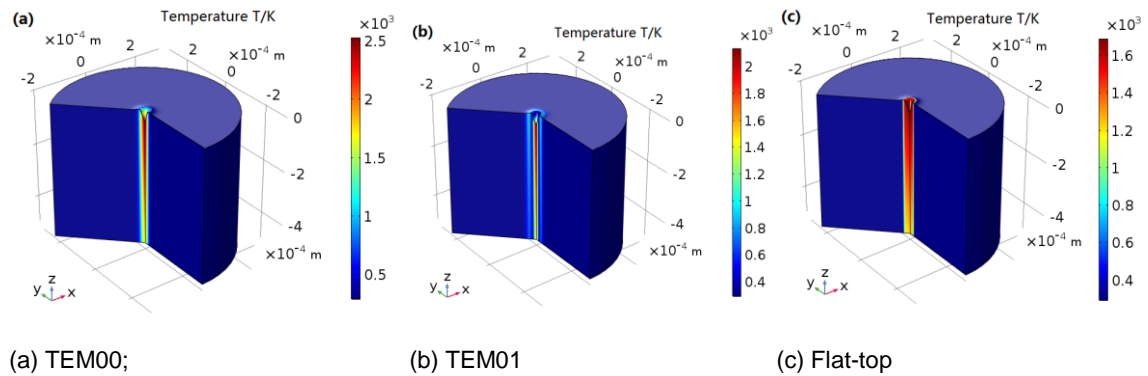


Figure 2: Temperature distribution of fused silica under different modes of beam irradiation

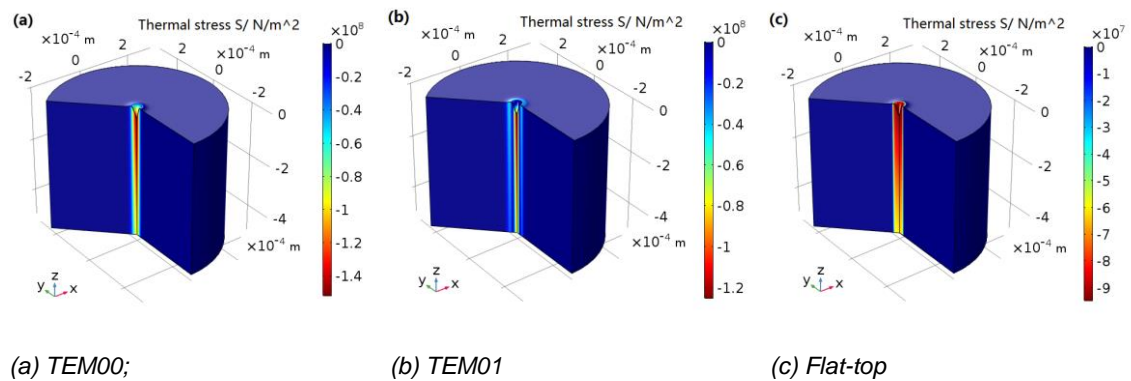


Figure 3: Thermal stress distribution of fused silica irradiated by different modes of light beams

The temperature of the fused silica micropores after TEM00, TEM01, and Flat-top three modes of laser irradiation and the distribution of thermal stress are shown in Figure 2 and Figure 3. From the simulation results, it can be seen that the surface temperature distribution of the micropores in the radial direction is basically consistent with the spatial distribution of the laser light intensity, and the temperature distribution gradually decreases with the depth inside the silica. The thermal stress distribution is similar to the temperature distribution. A positive value means that the thermal stress is a compressive stress, and a negative value means that the thermal stress is a tensile stress.

4.2 Temperature and thermal stress distribution of fused silica points

Three modes, TEM00, TEM01, and Flat-top were used for the laser irradiation, by simulation calculation we can get temperature and thermal stress curves at corresponding sampling points. Figure 4(a) shows that the temperature change curve at each sample point is similar to the integral curve of the laser pulse time distribution curve. The temperature rises significantly during the first half cycle of the laser pulse; at the same time, heat is accumulated due to the heat not being transferred to the surroundings in time. The arrival of the latter laser pulse keeps the temperature of the silica rising. Due to the different spatial distribution of light intensity, the temperature rise at point C under TEM01 mode laser irradiation is relatively slow, and the temperatures at point A, B, and C in the flat-top mode laser irradiation are very close in the rising process.

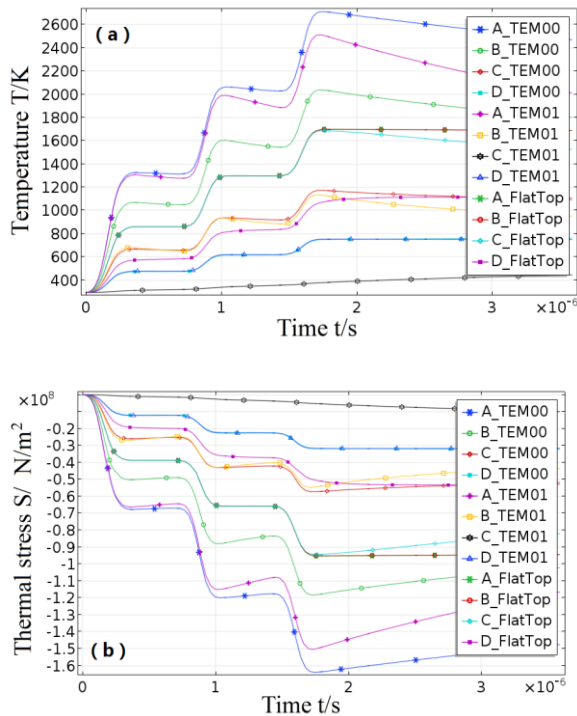


Figure 4: (a) Sampling points temperature change (b) Sampling points thermal stress change

From Figure 4(b), it can be seen that the thermal stress at the sampling points under the action of the laser appears as tensile stress. The compressive strength of fused silica is 1100MPa, the tensile strength is 48MPa, if the thermal stress exceeds the tensile strength of the material, it will lead to the fracture of the material. When the pulse is applied to fused silica, the temperature will continue to rise as the pulse continues to increase, which will cause the material to melt and vaporize, resulting thermal damage to the material. Although it is not enough to melt or vaporize the material in the lower temperature region, if the generated thermal stress exceeds the tensile strength of the material, the material will also break and fail.

5. Conclusions

The multi-physics simulation tool COMSOL was used to simulate the interaction between laser and fused silica, and the simulated data of three modes of laser-irradiated fused silica micropores were obtained. The simulation results show that: due to the different laser modes and micropores morphology, the damaged regions are different; on the one hand, the damage to the material comes from the temperature, when the

temperature reaches the material melting or vaporization temperature, it will lead to the melting and vaporization of the material; on the other hand, the damage comes from thermal stress, the temperature rise of the material is not uniform, so the huge temperature gradient leads to the generation of thermal stress, and the generated thermal stress reaches the mechanical failure threshold of the material, which causes thermal stress damage, and generates cracks and other morphologic damages.

References

- Cai J.X., Zhang Y., Wang D., 2014, Numerical Simulation Study on Thermal Stress Damage in 1064nm Anti-Reflection Fused Silica by Laser, *Journal of Changchun University of Science and Technology (Natural Science Edition)*, 37, 77-81.
- COMSOL Co., Ltd., 2013, *Structural Mechanics Module User's Guide*, Sweden.
- Feit M.D., 2002, Mechanisms of CO₂ laser mitigation of laser damage growth in fused silica, *Proceeding of SPIE*, 4932, 91-102.
- Gao Y.H., 2011, Research on beam shaping for high-order Gaussian Beam, *Optics & Optoelectronic Technology*, 9, 61-64.
- Grigoropoulos C.P., 2009, *Transport in Laser Microfabrication*, Cambridge University Press, New York, USA, 60-84.
- Jian Y., 2012, PhD Thesis, University Electronic Science and Technology of China, Chengdu, China
- Jiao J.K., Wang X.B., 2007, Temperature distribution of moving quartz glass heated by CO₂ laser, *High Power Laser and Particle Beams*, 19, 1-4.
- Li S.X., 2016, Research on the temperature and thermal stress of fused silica irradiated by a laser pulse, *LASER & INFRARED*, 46, 786-791. DOI: 10.3969/j.issn.1001-5078.2016.07.002
- Li Y., 2012, PhD Thesis, Department of Precision Instrument and Optoelectronic Engineering, Tianjin University, Tianjin, China.
- Norton M.A., 2004, Growth of laser initiated damage in fused silica at 1053 nm, *Proceeding of SPIE 2004*, Vol.5647, 197-205.
- Su L., Zeng X. D., 2009, Study of Thermal Deformations of Laser Windows, *Electronic Science and Technology*, 22, 63-65.
- Suratwala T.I., 2011, HF - Based Etching Processes for Improving Laser Damage Resistance of Fused Silica Optical Surfaces, *Journal of the American Ceramic Society*, 49, 416-428.
- Wei C.Y., He H.B., Deng Z., 2005, Study of thermal behaviours in CO₂ laser irradiated glass. *Optical Engineering*, 44(4), 044202
- Yoshida K., 2012, Influence of beam spatial distribution on the laser damage of optical material, *J Appl Phys*, 49, 3815-3819.
- Yu J.X., 2012, Simulation on stress control of laser irradiated fused silica on ANSYS, *Journal of University of Electronic Science and Technology of China*, 41, 870-874, DOI: 10.3969/j.issn.1001-0548.2012.06.011.